References

1. Singh, R. K.; Narayan, J. *Phys. Rev. B* **1990**, *41*, 8843.
2. Zheng, J. P.; Ying, Q. Y.; Witanachchi, S.; Huang, Z. Q.; Shaw, D. T.; Kwok, H. S. *Appl. Phys. Lett.* **1989**, *54*, 954.
3. Geohegan, D. B. In *Pulsed Laser Deposition of Thin Films*; Chrisey, D. B.; Hubler, G. K. Ed.; Wiley-Interscience: New York, U. S. A., 1995.
4. Polo, M. C.; Cifre, J.; Sanchez, G.; Aguiar, R.; Varela, M.; Esteve, J. *Appl. Phys. Lett.* **1995**, *67*, 485.
5. Amoruso, S.; Berardi, V.; Bruzzese, R.; Capobaianco, R.; Velotta, R.; Armenante, M. *Appl. Phys. A* **1996**, *62*, 533.
6. Park, S. M.; Shin, K. B.; Kim, Y. M. *Bull. Kor. Chem. Soc.* **1996**, *17*, 416.
7. Stritzker, B.; Pospieszczyk, A.; Tagle, J. A. *Phys. Rev. Lett.* **1981**, *47*, 356.
8. Wolf, P. J. *Appl. Phys. A* **1996**, *62*, 553.
9. Vega, F.; Afonso, C. N.; Solis, J. *J. Appl. Phys.* **1993**, *73*, 2472.
10. Gonzalo, J.; Vega, F.; Afonoso, C. N. *Thin Solid Films* *1994*, *241*, *96*.

Structural Phase Transformation of Layered Hydroxy Double Salts, $Ni_{1-x}Zn_{2x}(OH)_2(CH_3COO)_{2x} \cdot nH_2O$, Depending on Hydration Degree

Jin-Ho Choy*, Young-Mi Kwon, Seung-Wan Song, and Soon Ho Chang †

Department of Chemistry, Center for Molecular Catalysis, Seoul National University, Seoul 151-742, Korea
†Electronics and Telecommunications Research Institute, Taejon 305-600, Korea

Received January 9, 1997

There have been considerable interests in anion-exchangeable layered compounds such as layered hydroxy double salts (HDSs) and layered double hydroxides (LDHs) due to their potential applications to catalysts and ion exchangers.[1,2] The HDSs have a typical chemical composition of $[(M^{2+}N^{2+})_x(OH)_6(A^{m-})_{2/m}] \cdot nH_2O$ (M=Ni, Co, Zn in octahedral sites, N= Cu, Zn in tetrahedral sites) where A is the exchangeable anion such as Cl^-, NO_3^-, etc.[3,4] In this structure of HDSs, one quarter of octahedral sites in hydroxides layer planes are vacant at a maximum and divalent metal cations tetrahedrally coordinated are stabilized just below and above the empty octahedral sites, which leads to the creation of excess positive layer charge, contrary to LDHs where the surplus layer charge is formed by a partial substitution of trivalent cations for bivalent ones in octahedral sites. Overall charge neutrality is kept on by the presence of exchangeable anions which compensate positive layer charges in the interlayer space. So the structural stability is mainly based upon the electrostatic interaction between layers and anions as well as the hydrogen bonding network among interlayer anions, water molecules, and intralayer hydroxyl groups. In the present study, efforts have been made to investigate the intra- and inter-layer structures of the $Ni_{1-x}Zn_{2x}(OH)_2(CH_3COO)_{2x} \cdot nH_2O$ system,[5] and to discuss the influence of electrostatic interaction between host and guest on the structure. And at the same time, a new route to acetate intercalated HDSs has been proposed, since it is expected to be a good precursor for topotactic anion exchange reaction.

Experimental

Two samples of $Ni_{1-x}Zn_{2x}(OH)_2(CH_3COO)_{2x} \cdot nH_2O$ could be obtained from nickel-zinc mixed acetate solution by hydrothermal and coprecipitation routes. The concentration of nickel acetate and zinc one in the mixed solution was 0.06 M and 0.04 M, respectively, corresponding to x =0.25 in $Ni_{1-x}Zn_{2x}(OH)_2(CH_3COO)_{2x} \cdot nH_2O$. The mixed solution was hydrothermally treated at 150 °C for 48 hours under the pressure of 50 atm (hereafter, HT). The resulting green precipitate was separated by centrifuging, washing with decarbonated water, and drying at room temperature. In the coprecipitation (hereafter, CP), this mixed solution and the NH_4OH solution (10 wt.%) were dropwisely added to a flask containing 100 mL of decarbonated water at room temperature. The addition rate of the NH_4OH solution was adjusted to keep pH of the reaction mixture at 9.5. The pH value is included in the optimum synthetic condition of pH= 9-12 determined from logarithmic volubility isotherms as shown in Figure 1.[6,7] The volubility diagram is calculated from the thermodynamic equilibrium constants of nickel and zinc species in aqueous acetate solution listed in Table 1.[8] In the pH condition with same solubilities of $Ni(OH)_2$ and $Zn(OH)_2$, it is expected that the chemical composition of coprecipitate becomes homogeneous and controllable. Therefore, the optimum coprecipitation condition must be determined in the pH domain where both solubilities are the same approximately. In the whole experiments, nitrogen gas was constantly purged into reaction solution to prevent from carbonate contamination. The coprecipitate was aged at 60 °C for 15 hours and separated by centrifuging and washing with decarbonated water, and then dried at room temperature. The final products will be denoted henceforth as HT(t) and CP(t) with air-drying times, t minutes, under relative humidity of 60% at 25 °C. Their powder X-ray diffraction patterns were obtained by Phillips PW 3710 dif-

*To whom all correspondence should be addressed.

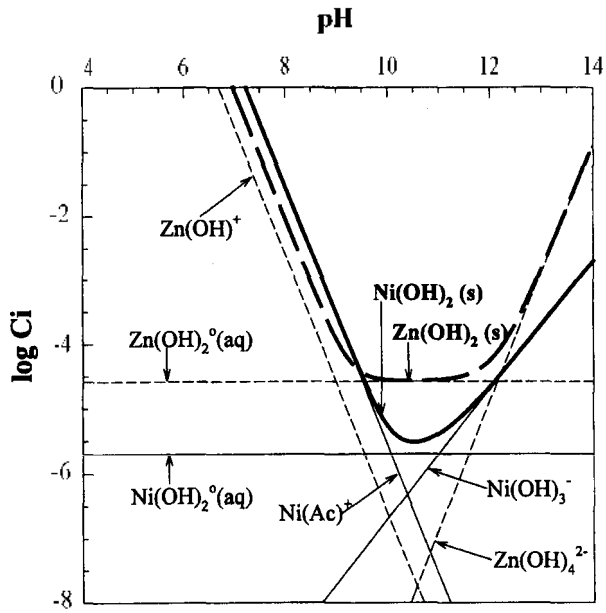

Figure 1. Solubility isotherms for nickel and zinc hyroxides in Ni(II)/Zn(II)-H_2O acetate system as a function of pH at 25 °C.

Table 1. Equilibrium constants of Ni(II)/Zn(II)-H_2O-acetate system at 25 °C[2]

Equilibrium reaction	log K
$Ni^{2+}+OH^- \rightarrow Ni(OH)^+$	4.1
$Ni^{2+}+2OH^- \rightarrow Ni(OH)_2°(aq)$	9.0
$Ni^{2+}+3OH^- \rightarrow Ni(OH)_3^-$	12.0
$2Ni^{2+}+OH^- \rightarrow Ni_2(OH)^{3+}$	3.3
$4Ni^{2+}+4OH^- \rightarrow Ni_4(OH)_4^{4+}$	28.3
$Ni^{2+}+2OH^- \rightarrow Ni(OH)_2(s)$	17.2
$Zn^{2+}+OH^- \rightarrow Zn(OH)^+$	5.0
$Zn^{2+}+2OH^- \rightarrow Zn(OH)_2(aq)$	11.1
$Zn^{2+}+3OH^- \rightarrow Zn(OH)_3^-$	13.6
$Zn^{2+}+4OH^- \rightarrow Zn(OH)_4^{2-}$	14.8
$2Zn^{2+}+OH^- \rightarrow Zn_2(OH)^{3+}$	5.0
$Zn^{2+}+2OH^- \rightarrow Zn(OH)_2(s)$	15.5
$Zn^{2+}+CH_3COO^- \rightarrow Zn(CH_3COO)^+$	1.57
$Zn^{2+}+2CH_3COO^- \rightarrow Zn(CH_3COO)_2$	1.36
$Zn^{2+}+3CH_3COO^- \rightarrow Zn(CH_3COO)_3^-$	1.57

fractometer with Ni-filtered Cu K- α radiation (λ =1.5418 Å). Thermogravimetry and differential thermal analyses (TG-DTA) were performed to investigate their thermal behavior and to determine the amount of interlayer water using Rigaku TAS-100 in the temperature range of 25-600 °C with a heating rate of 5 K/min in air. To determine the contents of acetate, nickel and zinc, elemental analyses were carried out by using Carlo Erba EA 1108 CHN analyzer and ICPS-5000 (SHIMAZU) ICP spectrometer. The FT-IR spectra were obtained using KBr disk method on a Bruker IFS 48 FT-IR spectrometer.

Results and Discussion

According to the X-ray diffraction patterns as shown in Figure 2, three (00 *l*) peaks and two large asymmetric bands

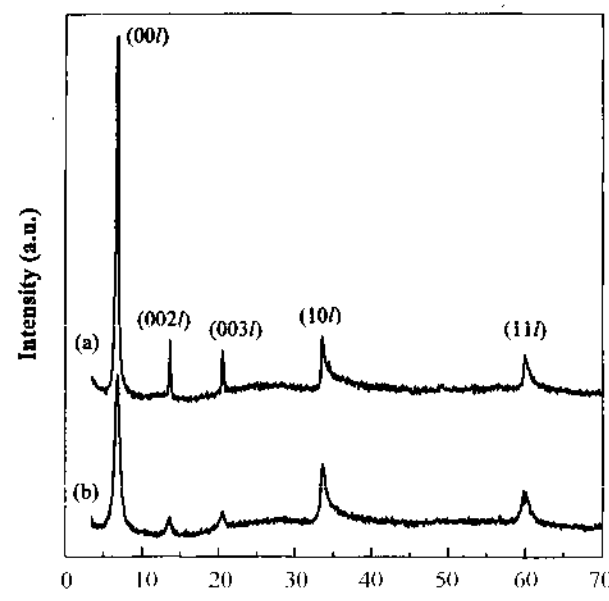

Figure 2. Powder X-ray diffraction patterns for (a) CP(60) and (b) HT(60).

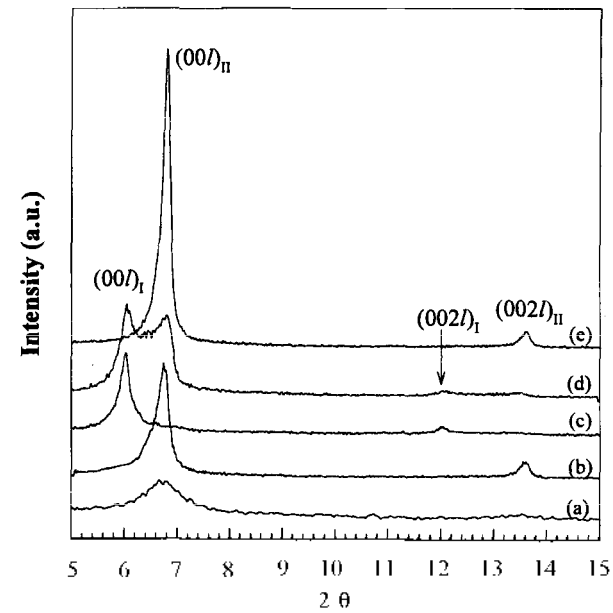

Figure 3. Evolution of X-ray diffraction patterns with respect to hydration rate for (a) CP(0), (b) CP(60), (c) HT(0), (d) HT(10), and (e) HT(60).

have been observed for both CP and HT samples. Such a pattern shows the formation of periodic disorder along the (10 *l*) and (11 *l*) planes of hydroxides layer, indicating the turbostratic layer structure. Subtracting the double hydroxides layer thickness of 4.6 Å from the basal spacing obtained by (00 *l*) peaks, it represents the interlayer distance of about 9 Å indicating that acetate anions are stabilized in the interlayer space.

The hydrothermally prepared sample (HT(t)) with different air-drying times shows interestingly the evolution of (00 *l*) peaks unlike CP(t) as shown in Figure 3. The (00 *l*) reflection for HT(0) is observed at 6.1° (d=14.5 Å), hen-

ceforth (00 *l*)$_1$ peak. However, upon drying in air, a new (00 *l*)$_2$ peak at 6.8° (d=13.0 Å) begins to appear at the expense of the peak at 6.1° and no further change in basal spacing could be observed after air-drying for an hour. As HT(60) was rehydrated, its interlayer distance was recovered to 14.5 Å. Therefore, the phase transformation in HT(t) is reversible, showing the critical role of water in the expanded layer structure of HT(0). However, in spite of such a drastic evolution of (00 *l*) peaks, the position and shape of two broad asymmetric bands corresponding to (10 *l*) and (11 *l*) planes are remained unchanged upon air-drying.

If two broad asymmetric bands are assumed to a local distortion within each slab, the deintercalation of interlayer water molecules should generate intralayer structural strains and modify the shape of two broad asymmetric bands. Therefore, the unchanged asymmetric bands upon the drying in air are resulting from a turbostratic character within each slab of HT(0) rather than a local distortion. The change of (00 *l*) peaks for HT(t) with respect to air-drying time is ascribed to the hydration rate of HT(t), which could modify the interlayer structure, but not the intralayer structure. At this point, it would be very interesting to understand the correlation among crystal structure of the host HDSs, orientation of the intercalated acetates, and content of the interlayer water.

In order to get an information on the interlayer molecular structures, the FT-IR spectra have been recorded for each sample. The characteristic doublet formed by two strong bands at about 1576 cm^{-1} and 1420 cm^{-1} assigned as $\nu_{asym}(CO_2)$ and $\nu_{sym}(CO_2)$ represents the interlayer acetate anions. No trace impurity of carbonate detected by the absence of $\nu_1(CO_3)$ band at 1384 cm^{-1}, is comparable to the acetate intercalated LDHs, since the parasitic carbonate inserted LDHs are always obtained under the same preparation conditions. Thus, the acetates in HDSs are more strongly captured by the zinc cations than in LDHs where they are randomly distributed in interlayer space.

To investigate the relation between the evolution of basal spacing and the orientation mode of acetate, the FT-IR spectra have been taken for each air-drying state of HT, HT(0), HT(10) and HT(60) and CP, CP(0), CP(60) as shown in Figure 4. Only the spectral domain of 1200-1800 cm^{-1} is presented since the orientation and coordination of acetate anions in the interlayer space can be deduced from the IR spectra in this carboxylate region.[9,10] The vibration modes of carboxyl group, in particular, $\nu_{asym}(CO_2)$, $\nu_{sym}(CO_2)$ and their difference in wave numbers (Δ) are critically affected by the orientation of inserted acetates, those which for HT series exhibited distinct variation.

The band frequencies of $\nu_{asym}(CO_2)$ and $\nu_{sym}(CO_2)$ for HT (0) is 1565 and 1420 cm^{-1}, respectively, but in the case of HT(60), they are observed at 1576 and 1417 cm^{-1}. On the other hand, the band frequencies of CP(t) series are the same with those of HT(60) with no shift along the hydration rate. Compared with those for references, acetate coordinated zinc complexes with classified orientation mode of acetate; unidentate ($\nu_{asym}(CO_2)$=1577 cm^{-1}, $\nu_{sym}(CO_2)$= 1420 cm^{-1}), chelating (1550 and 1405 cm^{-1}) and bridging (1639 and 1489 cm^{-1}), they assign to the orientation of acetate in each material as chelating for HT(0) and unidentate for HT(60) and CP(t) series.[9,10]

From no change in IR band frequencies for the CP(t) series, it is confirmed that the orientation of acetates is changed in accordance with the phase transformation of HT(t) as

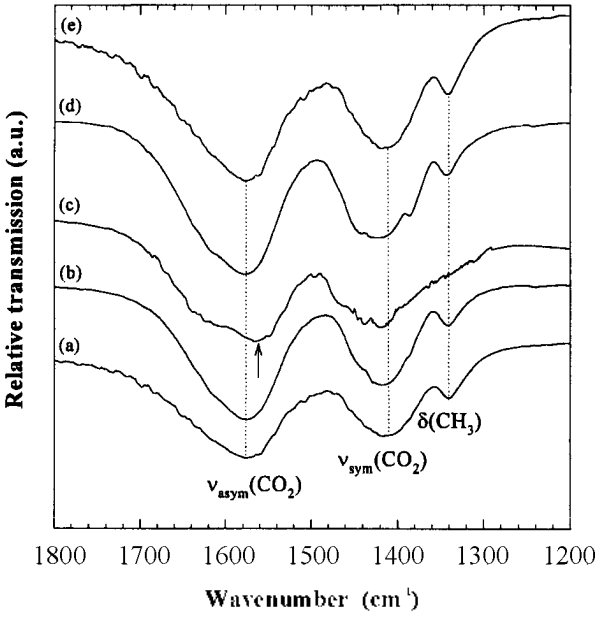

Figure 4. FT-Infrared spectra with respect to hydration rate in the 1200-1800 cm^{-1} range for (a) CP(0), (b) CP(60), (c) HT(0), (d) HT(10), and (e) HT(60).

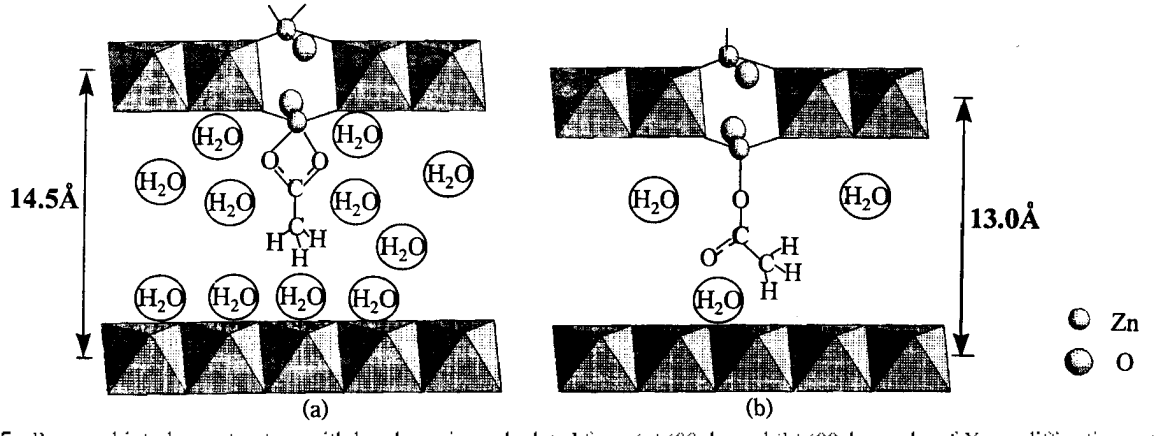

Figure 5. Proposed interlayer structure with basal spacing calculated from (a) (00 *l*) and (b) (00 *l*)$_2$ peaks of X-ray diffraction patterns.

shown in XRD analysis. The orientation of acetate for HT(0) would be chelating-type. However, the acetate for HT(60) might be ligated to the zinc cation with unidentate type orientation and the calculated basal spacing from this orientation (12.8 Å) matches very well with the experimental one of 13.0 Å from the XRD analysis.

Therefore, it is concluded that the phase transformation reported in the XRD analysis is corresponding to the change in orientation of inserted acetate depending on the hydration rate. That is, deintercalation of water molecules in interlayer gives rise to the rotation and arrangement of acetates themselves into their stable structure of unidentate in a given hydration condition as shown in Figure 5. The lower wavenumber position of $\nu_{asym}(CO_2)$ band in HT(0) is due to the decrease of asymmetry in two C-O bonds, which could be induced from the steric hindrance and hydrogen bonding of water molecules in the more hydrated condition.

In TG-DTA for HT(60) and CP(60), a similar thermal behavior could be observed. The weight loss up to 150 °C (12 wt.%) corresponds to the removal of interlayer water molecules, which was confirmed by a decrease of 3 Å in the basal spacing. The basal spacing was increased again progressively when the samples were cooled down to room temperature and kept on in air at relative humidity of 60%. The phenomenon indicates the reversible deintercalation and intercalation of interlayer water molecules in the temperature range of 25-150 °C. Beyond 280 °C, the host LDSs readily decomposes itself along with a strong exothermic decomposition of interlayer acetates.[11]

According to the relative atomic ratios from the results of ICP and CHN analyses, and water content from thermogravimetric analyses, formulas could be proposed to be $Ni_{0.32}Zn_{0.36}(OH)_2(CH_3COO)_{0.30}(OH)_{0.06}(H_2O)_{0.98}$ for HT(60) and $Ni_{0.74}Zn_{0.42}(OH)_2(CH_3COO)_{0.42}(OH)_{0.16}(H_2O)_{1.10}$ for CP(60), respectively.

The supplementary hydroxyl groups are included to the interlayer space for satisfying the charge neutrality. The nominal Zn/Ni ratio, as in the starting nickel-zinc mixed acetate solution, is maintained only for the CP sample. This gives a good reliability to our theoretical volubility diagram used in the coprecipitation method. The structural stability of CP regardless of hydration rate is obviously due to higher layer charge (x =0.26), compared to HT (x =0.18), resulting in a stronger electrostatic interaction between layers.

Acknowledgment. This research was in part supported by the Korean Science and Engineering Foundation through the Center for Molecular Catalysis, and by the Electronics and Telecommunications Research Institute.

References

1. Reichle, W. T. *J. Catal.* **1985,** *94,* 547.
2. Meyn, M.; Beneke, K.; Lagaly, G. *Inorg. Chem.* **1993,** *32,* 1209.
3. **Stähin,** W.; Oswald, H. R. *Acta Crystallogr. Sec.* B. **1970,** *26,* 860.
4. Ghose, S. *Acta Crystallogr.* **1964,** *17,* 1051.
5. Yamanaka, S.; Ando, K.; Ohashi, M. *Proc. Mat. Res. Symp.* **1995,** 371.
6. Choy, J. H.; Han, Y. S.; Kim, J. T.; Kim, Y. H. *J. Mater. Chem.* **1995,** *5,* 57.
7. Choy, J. H.; Han, Y. S.; Song, S. W.; Chang, S. H. Y. *Mater. Chem.* **1994,** *4,* 1271.
8. Martell, A. E.; Smith, R. M. In *Critical Stability Constants;* Plenum Press: New York, 1977.
9. Nakamoto, K. In *Infrared and Raman Spectra of Inorganic and Coordination Compound,* 4th ed.; John Wiley & Sons: New York, 1986, p. 232.
10. Deacon, G. B.; Phyllips, R. J. *Coord. Chem. Rev.* **1983,** *33, 227.*
11. Constantine, U. R. L.; Pinnavaia, T. J. *Inorg. Chem.* **1995,** *34,* 883.

Synthesis of New Chiral, C_2 Symmetric Receptors Containing Quaternary Ammonium Salts

Sung Keon Namgoong*, Ji Youn Hong, Ji-sook Lee, Kang-Bong Lee†, Ji-Hae Kwon, and Jung-Goo Lee‡

**Department of Chemistry, Seoul Women's University, Seoul 139-774, Korea*
Department of Chemistry, Korea Institute of Science & Technology, 130-650, Korea
†Kumho Chemical Laboratory, Taejon 305-348, Korea
Received January 31, 1997

Asymmetric synthesis by phase transfer catalysis using chiral ammonium salts has been extensively investigated by many groups.[1] The application of these catalysts has been mainly reported in the areas of chiral induction and kinetic resolution. However, in spite of their synthetic interest, most catalysts have proven to be ineffective in inducing asymmetry whereas the use of the catalysts derived from the naturally occurring cinchona alkaloids such as quinine, cinchonidine, etc. has been much more successful.[2,3]

Of several factors[4] influencing the Stereoselectivity in phase transfer reactions, the molecular structure of the catalyst seems to be the most important aspect: conformationally well-defined binding cavity sufficient to encapsulate appropriate substrates should be considered in the